THE ASTROPHYSICAL JOURNAL, 525:915–920, 1999 November 10

SPECTRUM SYNTHESIS OF ACCRETION DISKS IN PARTIAL ECLIPSE

RICHARD A. WADE[1] AND JEROME A. OROSZ[2]
Department of Astronomy and Astrophysics, Pennsylvania State University, 525 Davey Laboratory, University Park, PA 16802-6305
Received 1999 March 25; accepted 1999 July 2

ABSTRACT

We have modified a spectrum synthesis code for accretion disks in binary star systems, to deal with the case of a disk that is partially eclipsed by the mass-losing star. The known Roche geometry of the binary system permits the correspondence to be made between the spectrum observed over some phase interval and the regions of the disk that contribute to the spectrum. The code can generate simulated observations corresponding to arbitrary phase intervals, with arbitrary spectral sampling and resolution. This capability clearly includes generating broadband light curves as a limiting case. The use of angle-dependent specific intensities means that limb-darkening effects are automatically taken into account.

We present trailed-spectrogram and other representations of the partially eclipsed disk spectra of representative models of cataclysmic variables. The spectra are shown *versus* orbital phase, for portions of the ultraviolet spectral region accessible to the *Hubble Space Telescope*. We illustrate the behavior of blended features through eclipse and comment on the sensitivity of the synthesized spectra to the parameters of the input model, such as the stellar masses, mass transfer rate, and orbital inclination. Compared with out-of-eclipse spectra of the entire disk, observations during eclipse should have the advantage for diagnostic purposes of showing (1) deeper individual lines, (2) reduced blending of lines, and (3) an effectively smaller range of effective temperatures contributing to the observed spectrum. These advantages are especially important in analysis of the ultraviolet spectra of disks.

Subject headings: accretion, accretion disks — binaries: close — novae, cataclysmic variables — stars: atmospheres — ultraviolet: stars

1. INTRODUCTION

In most types of cataclysmic variable (CV) stars matter accretes onto the white dwarf via an accretion disk. In the more luminous classes of CVs the flux from the disk dominates the spectrum in the visible and ultraviolet (UV). Modern high-quality observations of CVs in the UV, e.g., observations by the *International Ultraviolet Explorer* (*IUE*) and the *Hubble Space Telescope* (*HST*), have demanded improved models of the photospheric line spectra of the accretion disks. Wade & Hubeny (1998, hereafter WH98) have presented examples of such improved models. The WH98 models are computed self-consistently in the plane-parallel approximation, assuming LTE and vertical hydrostatic equilibrium, by solving simultaneously the radiative transfer, hydrostatic equilibrium, and energy balance equations. Line transitions of elements from H to Ni are accounted for in the computation of the local spectra of individual disk annuli. Limb darkening, Doppler broadening, and blending of lines are fully accounted for in the computation of the integrated disk spectra.

In principle, one expects that the comparison of the WH98 models with high-quality, moderate-resolution UV spectra of novalike CVs would be a revealing exercise, since each absorption line is formed in a relatively narrow range of temperatures (and hence a narrow range of radii within the disk), and thus has a characteristic Doppler width. In practice, however, in whole-disk spectra the Doppler smearing of lines and also the dilution of lines by light from other zones in the disk make line features weak and hard to recognize, unless the disk is viewed nearly face-on. It is also rather difficult to obtain reliable measurements of the inclination and the mass of the white dwarf for CVs viewed nearly face-on, and as a result there is some uncertainty in choosing the proper WH98 models to compare with observations. In the present work, we show that *phase-resolved* spectroscopic observations of disks in eclipsing systems, interpreted with the aid of phase-resolved synthetic spectra, can provide useful diagnostic power. In contrast to the situation that is usual for a CV seen nearly face-on, the inclination and the mass of the white dwarf for eclipsing systems are often quite well determined. Since there is a smaller range of temperatures and projected velocities visible during partial eclipse phases, the observed spectrum does not suffer as much from Doppler smearing and line dilution.

These advantages of using observations of disks in phases of partial eclipse, outlined above, may turn out to be crucial in understanding whether actual disks are adequately described by simple theory or have unexpected features. Long et al. (1994), for example, found that it was not straightforward to interpret the energy distribution of the novalike variable IX Vel, obtained with the Hopkins Ultraviolet Telescope, using steady state models. Isolating regions of the disk for spectroscopic study by taking advantage of eclipsing geometries can be of use in measuring the $T_{\rm eff}(r)$ profile of the disk.

We describe below our modification to the WH98 models to account for eclipsing geometries, and we present examples of the appearance of the spectra through eclipse. The relation of this work to that of a similar effort by Linnell & Hubeny (1996) is also briefly discussed.

2. METHOD

The computation of a WH98 model spectrum involves four stages, which we summarize briefly (see WH98 for the detailed discussion). First, the disk is divided into concentric annuli which are independent plane-parallel radiating slabs. The vertical structure of each ring is computed with the program TLUSDISK (Hubeny 1990a, 1990b). (In WH98 and the present work, irradiation of the disk is not

[1] wade@astro.psu.edu.
[2] orosz@astro.psu.edu.

taken into account.) Second, the program SYNSPEC (Hubeny, Lanz, & Jeffrey 1994) is used to solve the radiative transfer equation to compute the local rest-frame spectrum for each ring. This computation includes typically thousands of lines selected from the list of Kurucz (Kurucz 1991; Kurucz & Bell 1995). Third, the program DISKSYN5a is used to combine the rest-frame intensities from all rings and generate the integrated disk spectrum. DISKSYN5a divides each ring into a large number of azimuthal sectors, and sums intensities from the individual elements with the appropriate area weighting and Doppler shifting (owing to the projected orbital motion of the gas within the disk). Finally, the program ROTINS is used to convolve the integrated disk spectrum with a Gaussian instrumental broadening function and resample the result uniformly in wavelength.

Our modification, to account for situations where the disk is partially eclipsed, is straightforward. (Linnell & Hubeny 1996 have presented an independent set of computer programs that accomplish a similar task. We compare our work with theirs below.) First, the mass and radius of the white dwarf are specified along with the mass transfer rate (or, equivalently, $T_{\rm max}$) and orbital inclination, in order to define a WH98 model. The Roche surfaces and the eclipsing geometry are then uniquely determined by further specifying the mass of the mass-losing secondary star and the orbital period or, equivalently, by specifying the mass ratio ($Q \equiv M_{\rm WD}/M_{\rm sec}$) and the orbital separation. We use a derivative of the Avni code (Avni & Bahcall 1975; Avni 1978; see also Orosz & Bailyn 1997) to compute the Roche lobe surfaces using a coordinate system that rotates with the binary. For a specified orbital phase, the coordinates of each surface element on the Roche lobe are then transformed onto a coordinate system in the plane of the sky, and the horizon of the secondary star is computed. Within DISKSYN5a, the coordinates of each surface area element of the disk are also transformed to the sky coordinates and are checked to see if they fall inside the projected horizon of the secondary. If a particular element is inside the horizon of the secondary, it is eclipsed and given zero weight as DISKSYN5a carries out the summation over sectors. (In the present implementation, the disk has zero thickness, i.e., it is assumed to be a flat object in the orbital plane of the binary.) ROTINS is used in the normal way after the modified DISKSYN5a step, to convolve the spectrum with an instrumental broadening profile and resample it.

The WH98 models do not include the contribution of the white dwarf to the total spectrum. The white dwarf may contribute a substantial amount of flux in the UV provided it is hot enough and either the mass of the white dwarf or the mass transfer rate is small enough. Our code computes the fraction of the white dwarf that is visible for a given geometry and phase, so it is straightforward to add a model spectrum of a white dwarf (with arbitrary rotation) to the model disk spectrum with the appropriate weighting. In practice, the white dwarf is usually either completely eclipsed or its upper hemisphere is fully visible (the opaque inner disk always blocks the lower hemisphere of the white dwarf)—the white dwarf eclipse ingress and egress phases last less than a few minutes for typical eclipsing CVs.

3. REPRESENTATIVE MODEL SPECTRA

To illustrate the appearance of the spectra through various eclipse phases, we choose the WH98 models *jj*, *dd*, *gg*, *bb*, and *k*. Models *jj* and *dd* have $M_{\rm WD} = 1.03\ M_\odot$ and $T_{\rm max} = 93{,}000$ K and 70,000 K, respectively. Models *gg*, *bb*, and *k* have $M_{\rm WD} = 0.55\ M_\odot$ and $T_{\rm max} = 52{,}000$, 39,000, and 29,000 K, respectively. For the illustrations we choose a secondary star mass of $M_{\rm sec} = 0.5\ M_\odot$ and an orbital period of 0.2 days. The inclinations chosen are $i = 74^\circ$ for models *jj* and *dd* and $i = 71^\circ$ for models *gg*, *bb*, and *k*. The masses and geometry for models *gg*, *bb*, and *k* are similar to those of the novalike system UX UMa (e.g., Baptista et al. 1995). In our illustrations we have omitted the light from the central white dwarf. Finally, we choose two different spectral resolutions at which to sample the final model spectra: $R = 25{,}000$ for models *jj* and *dd* (FWHM = 0.062 Å sampled every 0.0155 Å) and $R = 2000$ for models *gg*, *bb*, and *k* (FWHM = 0.78 Å sampled every 0.195 Å). The former resolving power was delivered by the G160M grating of the Goddard High Resolution Spectrograph (GHRS) aboard the *HST*, and the latter resolving power was delivered by the G140L GHRS grating.

Figure 1 shows the eclipse geometry and predicted spectra in the region of the Si II doublet ($\lambda\lambda = 1526.71$, 1533.45 Å) and C IV doublet ($\lambda\lambda = 1548.12$, 1550.76 Å) for

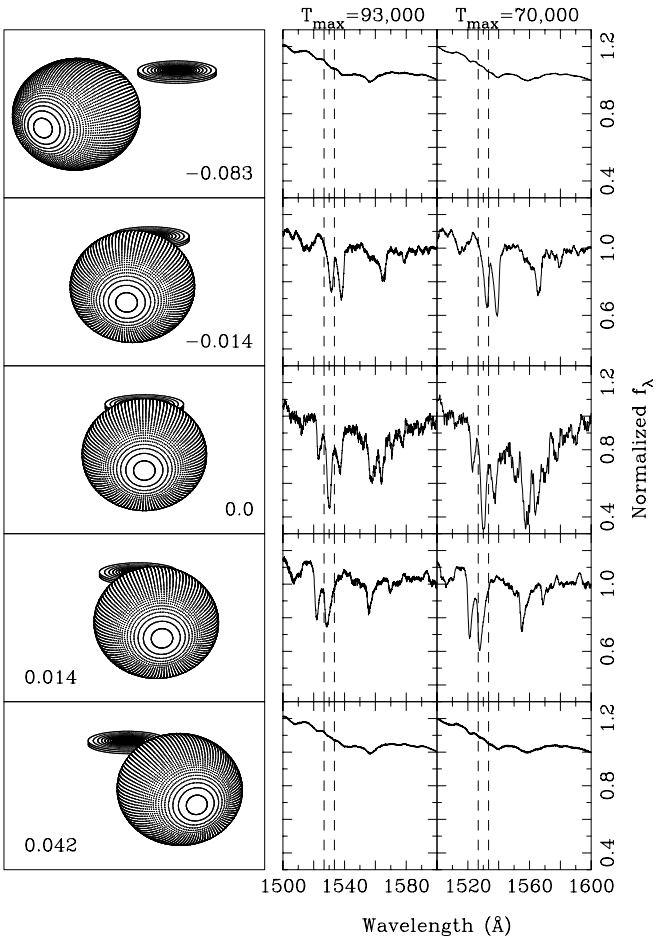

FIG. 1.—The eclipse geometry and predicted spectra for models *jj* ($T_{\rm max} = 93{,}000$ K) and *dd* ($T_{\rm max} = 70{,}000$ K) displayed for mass ratio $Q \equiv M_{\rm WD}/M_{\rm sec} = 2.06$ and inclination of 74°. The numbers in the left-hand panels indicate the orbital phase. The actual model disk is exactly in the orbital plane. For clarity in the presentation, we display the disk with a small thickness. We only show rings of the disk that have $T_{\rm eff} \gtrsim 10{,}000$ K. The normalized spectra (f_λ) are displayed in the rest frame of the white dwarf (i.e., the Doppler shifts owing to orbital motion around the binary center of mass are not included). The vertical dashed lines indicate the rest wavelength of the components of the Si II doublet.

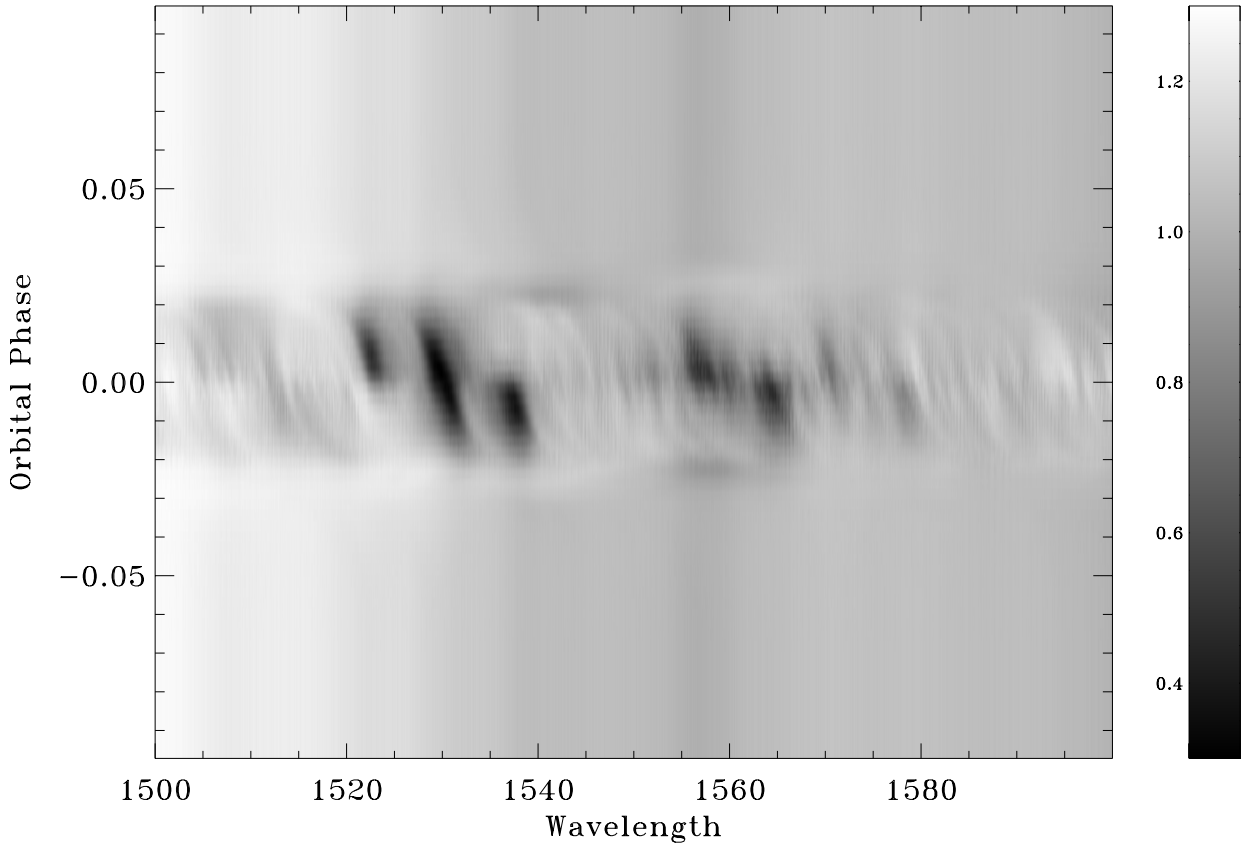

FIG. 2.—A "trailed" spectrum for model *jj* (T_{max} = 93,000 K) through eclipse (mass ratio 2.06 and inclination of 74°). The normalized spectra (f_λ) are displayed in the rest frame of the white dwarf (i.e., the Doppler shifts owing to orbital motion around the binary center of mass are not included). In this representation, darker colors indicate deeper lines.

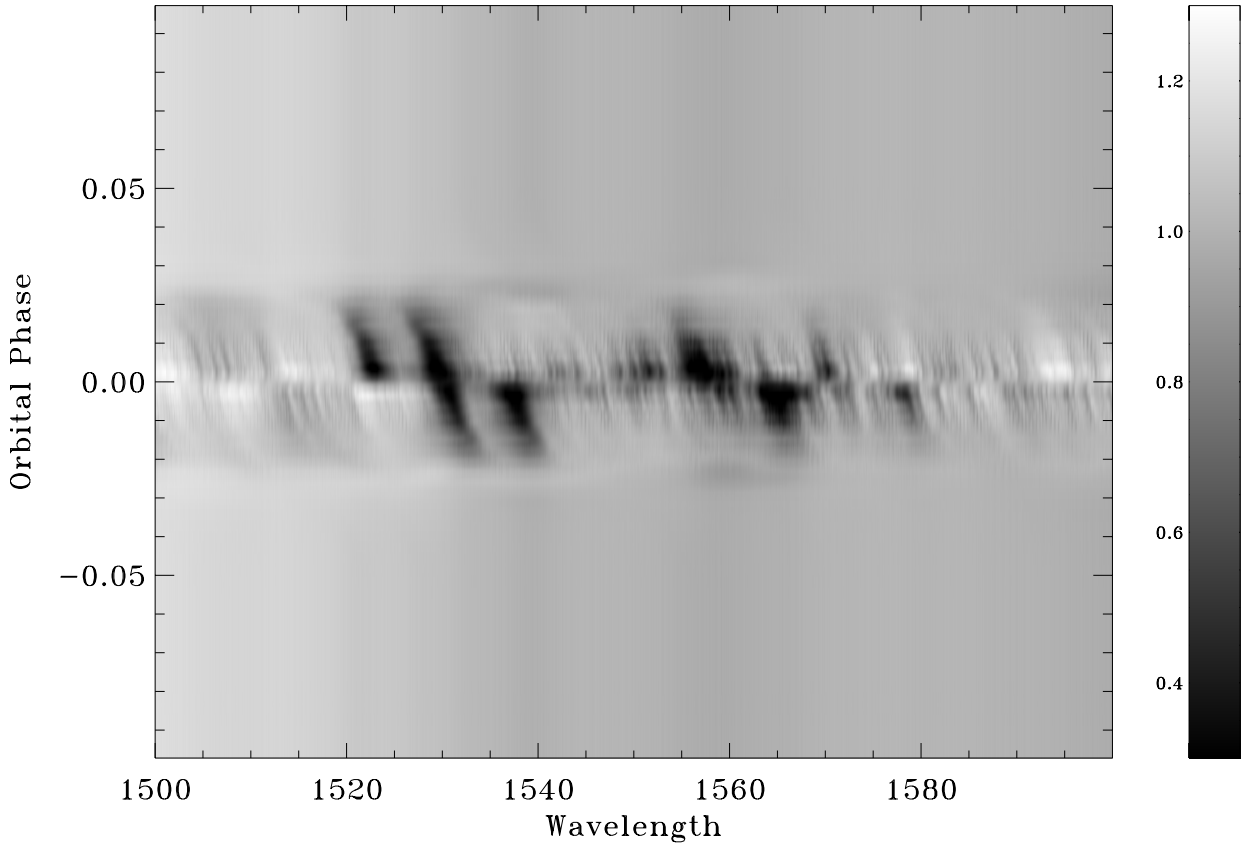

FIG. 3.—Similar to Fig. 2, with the "trailed" spectrum for model *dd* (T_{max} = 70,000 K) displayed

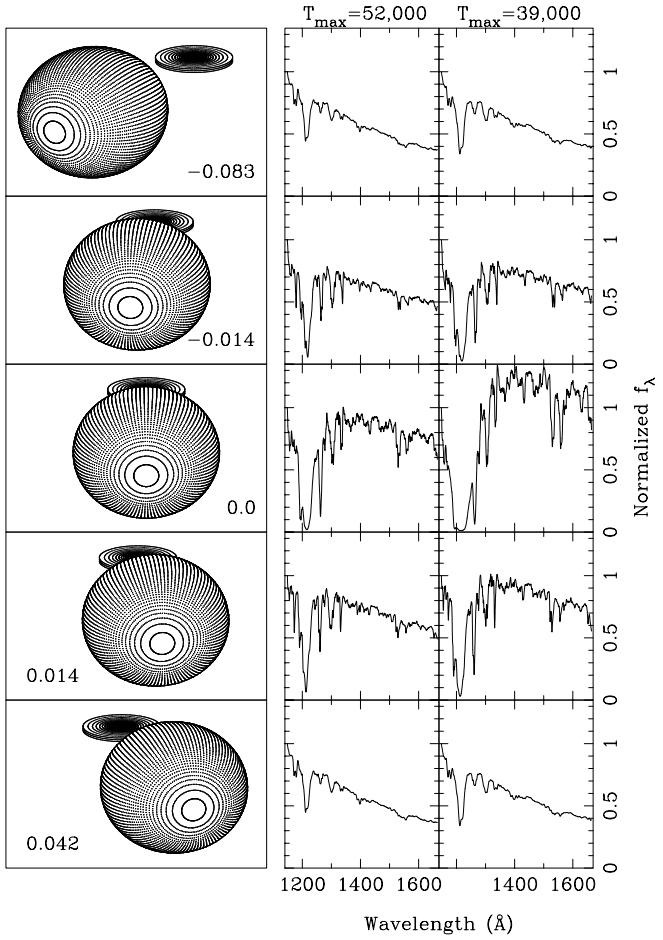

FIG. 4.—Similar to Fig. 1, with the eclipse geometry and predicted spectra for models *gg* (T_{max} = 52,000 K) and *bb* (T_{max} = 39,000 K) displayed for mass ratio $Q \equiv M_{WD}/M_{sec} = 1.1$ and inclination of 71°.

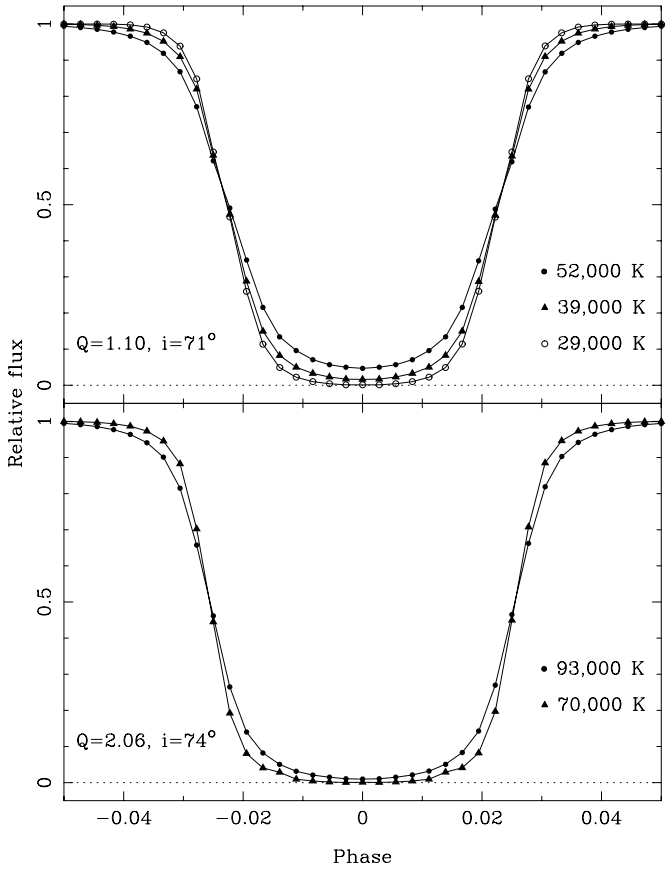

FIG. 5.—*Top*: The normalized continuum light curves for models *gg* (T_{max} = 52,000 K), *bb* (T_{max} = 39,000 K), and *k* (T_{max} = 29,000 K). Here the "continuum" is the average of the flux (f_λ) between 1440 and 1460 Å. The mass ratio is $Q \equiv M_{WD}/M_{sec} = 1.1$, and the inclination is $i = 71°$. *Bottom*: The normalized continuum light curves for models *jj* (T_{max} = 93,000 K) and *dd* (T_{max} = 70,000 K). Here the continuum is the average of the flux (f_λ) between 1585 and 1590 Å. The mass ratio is $Q = 2.06$, and the inclination is $i = 74°$.

models *jj* and *dd* at five different phases through the eclipse (mideclipse is phase 0.0). We display only the rings in the disk that have $T_{eff} \gtrsim 10{,}000$ K. For clarity each spectrum has been normalized at 1600 Å. Note that the spectra we show here are in the rest frame of the white dwarf—actual observed spectra would have an additional Doppler shift owing to the orbital motion of the star about its center of mass. It is straightforward to compute the appropriate radial velocities of each area element in the disk since the component masses, their separation, the orbital period, and the inclination are all specified.

The integrated disk spectra are almost featureless outside of eclipse. However, as the hotter inner regions of the disk are eclipsed, lines that are formed in the outer regions of the disk (for example, Si II) become apparent. The velocities of these lines depend on the orbital phase: they are redshifted just before mideclipse and blueshifted just after mideclipse. During mideclipse the lines have a mixture of red- and blueshifted components. Because the pattern of lines at mideclipse is different for models *jj* and *dd*, one may be able to distinguish between these two models in a real CV. Figures 2 and 3 showed "trailed" spectra for models *jj* and *dd* through the eclipse. The spectra are all normalized to unity at 1600 Å in order to emphasize line features. The patterns of the Doppler shifts and strengths of the lines as a function of the orbital phase are apparent from these figures. Finally, Figure 4 shows the eclipse geometry and predicted low-resolution spectra for models *gg* (T_{max} = 52,000 K) and *bb* (T_{max} = 39,000 K). The model spectra have been normalized to unity at 1148 Å. As before, the absorption lines become stronger during the eclipse.

In addition to the changes in the absorption-line pattern, strengths, and velocities, there is an obvious change to the continuum throughout the eclipse. Figure 5 shows continuum light curves for models *gg*, *bb*, and *k* (for a mass ratio of 1.1 and an inclination of 71°), and for models *jj* and *dd* (for a mass ratio of 2.06 and an inclination of 74°). As would be expected, for a fixed mass ratio and inclination, the shape of the eclipse profile depends on the maximum temperature of the disk. The hotter models have larger disks, i.e., the portion of the disk with $T_{eff} \gtrsim 10{,}000$ K is larger; there is little contribution in the UV from cooler zones. Thus the eclipse profiles of hotter models have longer ingress and egress durations and are not as deep. The continuum light curves can therefore in principle be used to distinguish between WH98 models with different values of the mass transfer rate $\dot{M}$, assuming that the mass of the white dwarf and the orbital inclination are known. Including light from the white dwarf will of course alter the contrast between eclipse minimum and out-of-eclipse light, as well as the detailed shape of the eclipse.

4. DISCUSSION

We have modified the codes of WH98 to account for situations where an accretion disk is partially eclipsed, using the correct geometry for Roche lobe filling stars. At a given partial eclipse phase, only those elements of the disk surface that are visible are summed to give the observable spectrum (each element of the disk is Doppler shifted by an appropriate amount). Because the spectra are constructed from detailed files of specific intensity, rather than angle-averaged flux, limb-darkening effects (e.g., Diaz, Wade, & Hubeny 1996) are automatically taken into account. The intensity files store the fully resolved, line-by-line rest-frame spectrum of the local disk atmospheres, and a synthetic spectrum can be generated with any final wavelength sampling interval and instrumental resolution desired (this includes broadband light curves in the limiting case).

We have shown that through eclipse, the model line spectra should vary greatly in character, revealing at various phases a succession of features, formed at different temperatures and with Doppler shifts that characterize the radius of formation. Phases near mideclipse, when the bright inner disk is occulted, will be especially interesting in revealing the line spectrum of the outer, cooler disk. There should be a pronounced "rotational disturbance" in the observed wavelengths of the features, depending on whether the approaching or receding side of the disk is visible. This will also help establish the distance from the white dwarf at which certain temperatures prevail. Thus it is possible in principle to infer the run of $T_{\rm eff}$ with radius and determine whether the disk is in a "steady state" (i.e., $T_{\rm eff} \propto r^{-3/4}$ roughly; Pringle 1981).

Because our approach allows us to compute the *phase-averaged* spectrum over some phase interval, it becomes possible to bin observed spectra from a time series to meet any desired signal-to-noise criterion and still make a direct comparison with the model spectra. This is important, for example, when considering RAPID mode observations with the *HST* GHRS or FOS instruments. By using this direct modeling approach, we avoid certain pitfalls of the maximum entropy–based (ME) eclipse mapping method that has been commonly used to analyze time series data of CVs (e.g., the study of UX UMa by Baptista et al. 1995). In the ME approach, the need to smooth the maps in azimuth (at least partially) means that narrow passbands suffer from contamination from out-of-band light that is mixed into the passband due to Doppler shifts, whereas passbands that are wide enough to avoid this problem fail to resolve the line spectrum adequately. Thus ME-based methods degrade the *spectral* information carried in spectroscopic time series of moderate resolution. Our direct approach avoids this difficulty—given the parameters of the binary system (the mass ratio, the orbital separation, and the inclination) and of the accretion disk (the mass of the white dwarf, its radius, and the mass transfer rate), we can produce a model spectrum at any resolution, corresponding to any interval in orbital phase. Adjusting the model to match the observations then provides a path to direct estimation of the CV parameters, provided of course that the steady state (or other) models adequately describe the actual structure and spectra of accretion disks.

We noted above that our figures and computations only take into account rings in the accretion disk that have $T_{\rm eff} \gtrsim 10{,}000$ K. If a large fraction of this part of the disk is eclipsed at a particular orbital phase, then it is of course necessary to take into account the flux from cooler zones of the disk, even in the ultraviolet. This would be necessary, for example, with the cooler disk models *h*, *j*, *s*, *t*, *u*, and *v* of the WH98 grid, if viewed with the same geometries as used in the figures, since the entire "hot" inner disk is occulted at phase zero for these cases.

Linnell & Hubeny (1996, hereafter LH96) have described a light curve and spectrum synthesis code for disks in binary systems, which is part of a more general implementation than the one we describe here, and which has a different heritage. While many of the details of implementation of course differ, there is an overall similarity in purpose, namely, to compute phase-dependent spectra and light curves for eclipsing close binary systems that contain an opaque accretion disk. The interested reader may consult Avni & Bahcall (1975), Avni (1978), and Orosz & Bailyn (1997) for the detailed heritage of our approach. It is not our intention to generalize our code to deal with the variety of situations contemplated by LH96, but to do so would mainly require attention to including the mass-losing star as a source of light; a more complete description of the vertical structure and outer rim of the disk, so as to allow computation of eclipses of the mass-losing star; and perhaps an internal treatment of irradiation, which would involve an iterative and dynamical reassignment of radii.

LH96 consider four components: the mass-gaining star, the mass-losing star, the disk, and the disk rim. We consider only the disk and the mass-gaining star, which is always compact (a white dwarf). The complexity of computing visibility of each light-emitting element is thus much reduced in our code.

LH96 consider a disk that has a finite vertical thickness and an outer rim, important considerations for the case of disks in Algol binaries, where the effective gravity in the disk is much less, and the opening angle of the disk is much greater, than in CVs. This modification for "flared" disks could be made without difficulty in our Avni-based code, to deal with cases of very nearly edge-on disks, using the self-consistently computed thickness of the disk as LH96 discuss. For CVs viewed at an inclination greater than about 80° this will be important, both in determining the "visibility" of each sector of the disk surface and in establishing the correct emergent angle from each sector along with the corresponding limb darkening (see Robinson, Wood, & Wade 1999 for a further discussion). The precise geometry of the outer disk is also important for calculating the spectrum and light curve at secondary eclipse (eclipse of the mass-donating star). This is an aspect of the general problem with which we are not concerned, since our emphasis is on understanding the disk in the ultraviolet, where it dominates and where the cool secondary star does not compete.

LH96 allow for the inner radius of the disk to be greater than the radius of the accreting star; this is an easy run-time modification to make with DISKSYN5a. Like LH96, we can easily adopt a $T_{\rm eff}(r)$ relation for the disk that differs from the usual steady state prescription, and this will be an important avenue to explore.

We have emphasized in our approach the ability to compute spectra of disks in partial eclipse over an arbitrary interval of orbital phase, by suitably averaging instantaneous spectra, in order to match the circumstances of observation. We have illustrated, using "trailed" spectra, the

complex behavior of the UV disk spectrum that makes this approach necessary.

5. SUMMARY

We have modified the WH98 spectrum synthesis code for accretion disks in binary star systems, to deal with the case of a disk that is partially eclipsed by the mass-losing star. The known Roche geometry of the binary system permits the correspondence to be made between the spectrum observed over some phase interval and the region of the disk that contributes to the spectrum. Our code can generate simulated observations corresponding to arbitrary phase intervals, with arbitrary spectral sampling and resolution. We use angle-dependent specific intensities, so limb-darkening effects are automatically taken into account. Compared with out-of-eclipse spectra of the entire disk, observations during eclipse are expected to have the advantage for diagnostic purposes of showing (1) deeper individual lines, (2) less blending of lines, and (3) an effectively smaller range of effective temperatures contributing to the observed spectrum. These advantages are especially important in analysis of the ultraviolet spectra of disks. We illustrate the potential diagnostic power of such data as might be obtained by the GHRS, using partially eclipsed model disk spectra for cases corresponding to realistic CV parameters.

Support from NASA grants NAGW-3171 and NAG5-3459 and from STScI grants GO-3683, GO-06661, and AR-07991 is gratefully acknowledged.

REFERENCES

Avni, Y. 1978, in Physics and Astrophysics of Neutron Stars and Black Holes, ed. R. Giacconi & R. Ruffini (Amsterdam: North Holland), 42
Avni, Y., & Bahcall, J. N. 1975, ApJ, 197, 675
Baptista, R., Horne, K., Hilditch, R. W., Mason, K. O., & Drew, J. E. 1995, ApJ, 448, 395
Diaz, M. P., Wade, R. A., & Hubeny, I. 1996, ApJ, 459, 236
Hubeny, I. 1990a, ApJ, 351, 632
———. 1990b, in IAU Colloq. 129, Structure and Emission Properties of Accretion Disks, ed. C. Bertout et al. (Gif-sur-Yvette: Editions Frontières), 227
Hubeny, I., Lanz, T., & Jeffery, C. S. 1994, St. Andrews Univ. Newsl. Anal. Astron. Spectra, 20, 30
Kurucz, R. L. 1991, in Stellar Atmospheres: Beyond Classical Models, ed. L. Crivellari et al. (Dordrecht: Kluwer), 441
Kurucz, R. L. & Bell, B. 1995, Kurucz CD-ROM 23, Atomic Line List (Cambridge: Smithsonian Astrophys. Obs)
Linnell, A. P., & Hubeny, I. 1996, ApJ, 471, 958 (LH96)
Long, K. S., Wade, R. A., Blair, W. P., Davidsen, A. F., & Hubeny, I. 1994, ApJ, 426, 704
Orosz, J. A., & Bailyn, C. D. 1997, ApJ, 477, 876
Pringle, J. E. 1981, ARA&A, 19, 137
Robinson, E. L., Wood, J. H., & Wade, R. A. 1999, ApJ, 514, 952
Wade, R. A., & Hubeny, I. 1998, ApJ, 509, 350 (WH98)